

pubs.acs.org/Biomac Article

# Supramolecular Hydrogels via Light-Responsive Homoternary Cross-Links

Lei Zou, Christopher J. Addonizio, Bo Su, Matthew J. Sis, Adam S. Braegelman, Dongping Liu, and Matthew J. Webber\*



Cite This: Biomacromolecules 2021, 22, 171–182



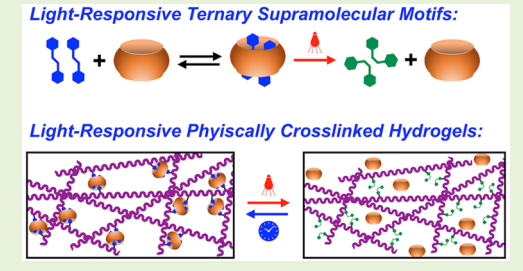
**ACCESS** 

Metrics & More



si Supporting Information

**ABSTRACT:** Host–guest physical cross-linking has been used to prepare supramolecular hydrogels for various biomedical applications. More recent efforts to endow these materials with stimuli-responsivity offers an opportunity to precisely tune their function for a target use. In the context of light-responsive materials, azobenzenes are one prevailing motif. Here, an asymmetric azobenzene was explored for its ability to form homoternary complexes with the cucurbit[8]uril macrocycle, exhibiting an affinity  $(K_{eq})$  of  $6.21 \times 10^{10}$  M $^{-2}$  for sequential binding, though having negative cooperativity. Copolymers were first prepared from different and tunable ratios of NIPAM and DMAEA, and DMAEA groups were then postsynthetically modified with this asymmetric azobenzene.



Upon macrocycle addition, these polymers formed supramolecular hydrogels; relaxation dynamics increased with temperature due to temperature-dependent affinity reduction for the ternary complex. Application of UV light disrupted the supramolecular motif through azobenzene photoisomerization, prompting a *gel-to-sol* transition in the hydrogel. Excitingly, within several minutes at room temperature, thermal relaxation of azobenzene to its *trans* state afforded rapid hydrogel recovery. By revealing this supramolecular motif and employing facile means for its attachment onto pre-synthesized polymers, the approach described here may further enable stimuli-directed control of supramolecular hydrogels for a number of applications.

## 1. INTRODUCTION

The design of supramolecular hydrogels affords opportunity to create new biomaterials and drug delivery devices with enhanced functionality. 1-4 In particular, by endowing macromer or polymer building blocks with macrocyclic hosts and/or their corresponding guests, physically cross-linked hydrogel networks can be formed through host-guest recognition and complex formation.<sup>5,6</sup> Many interesting properties arise from hydrogels prepared using these dynamic and reversible motifs, including a shear-thinning and self-healing capacity conducive to minimally invasive syringe injection, extrusion processing, or 3D printing.<sup>7,8</sup> The ability of a supramolecular hydrogel to autonomously form and/or self-heal in situ has several benefits as an injectable hydrogel compared to more conventional means of forming hydrogels in situ,9 some of which include radical-mediated covalent cross-linking schemes entailing monomers and/or free-radical (photo)initiators which may be toxic.  $^{10,11}$  Other routes have used more mild bioconjugation reactions to induce covalent cross-linking between building blocks, 12,13 though this approach often lacks orthogonality as there is a high concentration of various small molecule analytes and/or proteins which bear groups that can also react by some of the more common mechanisms. In addition, depending on the route of covalent bond formation via either radical-initiated or bioconjugation schemes, these may suffer from reaction kinetics which prove limiting in the face of convective flux in a tissue site of interest. By comparison, host—guest motifs can be formed with  $k_{on}$  near the diffusion limit, <sup>14</sup> enabling rapid restoration of physical cross-linking upon cessation of injection shearing. Other routes have leveraged the transition from ambient to physiologic temperature for hydrogelation, <sup>15</sup> offering a mild, autonomous, and reversible route to create materials through noncovalent interactions. Recently, routes capturing features of both host—guest supramolecular cross-linking and thermoresponsive gelation have been reported which take advantage of both dynamic and reversible host—guest physical cross-linking interactions as well as physiologic temperature stimuli. <sup>16,17</sup>

The creation of supramolecular hydrogels with properties responsive to external stimuli affords a means to control the function of a material and more fully recreate the "living" features of materials in the natural world. Light is a well-explored external stimulus in the context of supramolecular hydrogels given the ease with which the location and "dose" of irradiation can be controlled, and strategies have thus explored

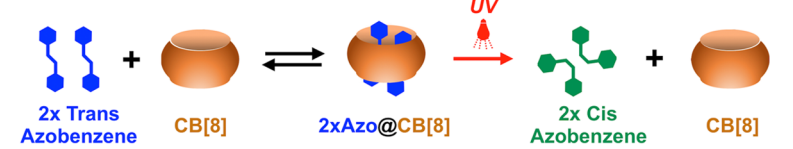
Special Issue: Bioinspired Macromolecular Materials

Received: June 21, 2020 Revised: July 29, 2020 Published: August 17, 2020





# A CB[8]-Azobenzene Homoternary Complex:



# **B** Physical Crosslinking of Azobenzene-Pendant Polymer:

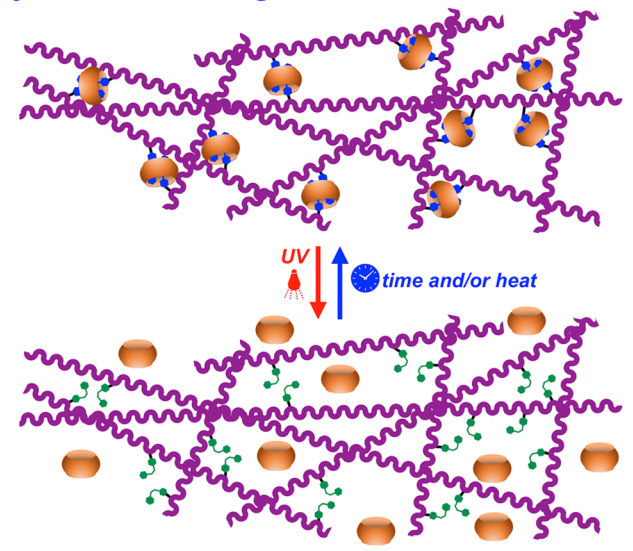


Figure 1. (A) Schematic illustrating the proposed route to use asymmetric azobenzene guests to facilitate homoternary (i.e., 2:1) complexes with CB[8]. Upon photoisomerization of the azobenzene guest, it no longer complexes with CB[8]. (B) Pendant presentation of the azobenzene guest from polymeric backbones is intended to facilitate physical cross-linking via homoternary complex formation with free CB[8]. Upon photoisomerization, these cross-links are then broken to induce a *gel-to-sol* transition and network dissipation. The cross-links can, in principle, recover depending on the relaxation rate of the azobenzene.

the use of light to alter affinity of a host-guest motif so as to modulate the properties of a bulk material. 21,22 The azobenzene family, which undergoes trans-cis photoisomerization with UV light, is among the most common of such guest motifs to be evaluated for response to an external stimuli. 23,24 The trans-isomer is typically the thermodynamically preferred state and has a dihedral angle between the two benzene rings of  $\sim 0^{\circ}$ . Upon irradiation with UV light (c.a., 365 nm), the cis isomer is formed, characterized as a more compact, threedimensional molecule with a dihedral angle between the two benzenes now out of plane at  $\sim 60^{\circ}$ ; irradiation with visible light (c.a., 430-550 nm) or mild heating typically enables cisto-trans relaxation to the preferred trans conformation. A number of responsive supramolecular hydrogels have thus been reported which leverage preferred recognition of transazobenzene guests by the cyclodextrin family of macrocycles.26-28

Cucurbit[n]urils (CB[n]) are an interesting family of synthetic macrocycles and though not as pervasive in their use as cyclodextrins, afford possible advantages due to their uncommonly high-affinity binding to a variety of guests. <sup>29,30</sup> One member of this family, CB[8], is able to form stable ternary complexes by simultaneously binding two different guests in its portal. <sup>31,32</sup> Sequential and cooperative binding of an electron-poor guest and an electron-rich guest has been shown as a useful strategy to create physically cross-linked hydrogels through heteroternary complex formation with free CB[8]. <sup>33,34</sup> Toward light-responsive CB[8] assemblies based

on azobenzenes, the heteroternary complex formation of a positively charged first guest (e.g., bipyridinium dication) with a typically uncharged azobenzene second guest has been explored.<sup>35–38</sup> The use of azobenzene motifs to create supramolecular hydrogels from CB[8] cross-linking has, however, not been reported; a report did use competition from a soluble azobenzene motif for light-mediated disruption of a CB[8] supramolecular hydrogel.<sup>39</sup>

Here, we explored homoternary complex formation of CB[8] binding two asymmetric azobenzene motifs simultaneously and evaluated this motif for the creation of supramolecular hydrogels physically cross-linked by CB[8]azobenzene ternary complexes to enable light-mediated disruption of physical cross-linking (Figure 1). Specifically, we report a new homoternary complex based on the photoresponsive azobenzene family of motifs and then integrate this cross-linking mechanism to create lightresponsive azobenzene cross-linked supramolecular hydrogels. The light-mediated trans-to-cis conversion of azobenzenes in these materials leads to gel dissipation via the disruption of supramolecular cross-links. An interesting discovery of rapid cis-to-trans relaxation for pendant azobenzene guests on the polymer at room temperature enables these hydrogels to recover within minutes of ceasing UV irradiation. While the enclosed study only establishes the utility of light-responsive ternary cross-linking in supramolecular hydrogels, there are a variety of biomaterial contexts for which this technique could be deployed to enable new responsive hydrogel platforms for

Scheme 1. Synthetic Scheme to Prepare AzoSM, along with the AzoBr Intermediate Used in Subsequent Steps for Polymer Modification

applications as transient and mechanically tunable cell substrates or for pulsed delivery of macromolecular therapeutics.

#### 2. EXPERIMENTAL SECTION

**2.1. Synthesis of AzoSM.** The synthetic route to a small molecule azobenzene derivative (AzoSM) entailed four steps (Scheme 1), as detailed below:

2.1.1. Synthesis of 4-Methylphenyldiazenylphenol. The synthesis of 4-methylphenyldiazenylphenol was performed according to a published protocol. $^{40}$ 

2.1.2. Synthesis of 4-Methylphenyldiazenylanisole. 4-Methylphenyldiazenylphenol (12.72 g) and  $K_2CO_3$  (12.42 g) were suspended and stirred together in acetone (200 mL) for 2 h under reflux.  $Me_2SO_4$  (4.26 mL) was then added to the suspension, and the reaction mixture was further refluxed for 4 h. Most of the acetone was removed under reduced pressure, and the residue was partitioned between hexane/dichloromethane (1:1, 200 mL) and water (200 mL). The organic phase was further washed with water (200 mL) twice and then evaporated under reduced pressure. The residue was recrystallized from MeOH to obtain orange crystals (7.85 g, 57.9% yield).  $^1H$  NMR (500 MHz Bruker, 25  $^\circ$ C, CDCl $_3$ , Figure S1):  $\delta$  (ppm) = 7.90 (m, 2H), 7.79 (m, 2H), 7.30 (m, 2H), 7.01 (m, 2H), 3.89 (s, 3H), 2.43 (s, 3H).

2.1.3. Synthesis of 4-Bromomethylphenyldiazenylanisole (AzoBr). 4-Methylphenyldiazenylanisole (7.85 g), NBS (6.20 g), and AIBN (285.0 mg) were refluxed in CCl<sub>4</sub> (150 mL) for 3 h. The reaction mixture was then diluted with 100 mL of hexane and washed with water (200 mL) two times. The organic layer was evaporated under reduced pressure to give an orange solid (10.70 g). From <sup>1</sup>H NMR, this orange solid was found to contain 90 mol % of 4-bromomethylphenyldiazenylanisole and 10 mol % 4-methylphenyldiazenylanisole. The orange solid was used directly for further steps without additional purification. <sup>1</sup>H NMR (500 MHz Bruker, 25 °C, CDCl<sub>3</sub>, Figure S1):  $\delta$  (ppm) = 7.92 (m, 2H), 7.85 (m, 2H), 7.52 (m, 2H), 7.02 (m, 2H), 4.56 (s, 2H), 3.90 (s, 3H).

2.1.4. Synthesis of N-4′-Bromomethylphenyldiazenylanisole-N,N,N-trimethylammonium bromide (AzoSM). 4-Bromomethylphenyldiazenylanisole (567.0 mg, 90% pure as noted above) and trimethylamine (0.44 mL of 4.2 M in MeOH) were dissolved in diethyl ether (20 mL), and the mixture was stirred for 24 h. An orange precipitate (670.0 mg, 100% yield) was collected by centrifuge and carefully washed three times with small amounts of ether.  $^1\mathrm{H}$  NMR (500 MHz Bruker, 25 °C, D2O):  $\delta$  (ppm) = 7.76 (m, 4H), 7.60 (d, 2H), 7.02 (d, 2H), 4.45 (s, 2H), 3.80 (s, 3H), 3.02 (s, 9H).

**2.2. Synthesis of CB[8].** Cucurbit[8]uril (CB[8]) was synthesized and purified according to previously reported methods.<sup>41</sup>

**2.3.** <sup>1</sup>H NMR Ternary Complex Assessment. To validate both photoisomerization of AzoSM and its ternary complex formation with CB[8], <sup>1</sup>H NMR was performed (500 MHz Bruker, 25 °C, D<sub>2</sub>O). The spectra for AzoSM (15 mM) was first collected, and it was subsequently irradiated within a Rayonet RPR-200 photoreactor (Southern New England Ultraviolet) equipped with a circumferential arrangement of 16 lamps (350 nm,  $\sim$  15 mW/cm<sup>2</sup>) for 5 min to drive

conversion to the *cis* form. The sample was placed on ice and immediately transferred back to the NMR for data collection. The same procedure was then performed for **AzoSM** (15 mM) with 0.5 eq of **CB[8]**, with measurements taken before and immediately after UV exposure.

**2.4. Isothermal Titration Calorimetry.** Isothermal titration calorimetry (ITC) was performed on a MicroCal PEAQ instrument equipped with a 40  $\mu$ L syringe. In total, 19 injections were made in all runs; the first injection of 0.4  $\mu$ L was discarded from data analysis, while the subsequent 18 injections were 2  $\mu$ L each in volume. Each experiment titrated **AzoSM** (300  $\mu$ M) into **CB**[8] (20  $\mu$ M) in DI water at 4, 20, and 37 °C, with background subtraction of a dilution control of **AzoSM** (300  $\mu$ M) into DI water at each of these temperatures. Three independent experiments were run for each temperature, and the data were fit to a sequential binding model (A+B+B  $\leftrightarrow$  AB+B  $\leftrightarrow$  ABB) through global analysis of all three runs by integrated use of public-domain software (NITPIC, Sedphat, GUSSI) following reported analysis methods. <sup>42</sup>

**2.5.** UV—vis Relaxation Kinetics. The kinetics of cis-to-trans relaxation of azobenzenes were also assessed using UV—vis absorbance spectroscopy using a Tecan M200 microplate reader. The relaxation of AzoSM (0.15 mM) was studied with and without addition of 0.5 eq CB[8]. An initial spectrum in the *trans* state was collected, and the sample was then irradiated within a Rayonet RPR-200 photoreactor (Southern New England Ultraviolet) equipped with a circumferential arrangement of 16 lamps (350 nm, ~15 mW/cm²) for 5 min to drive conversion to the *cis* form. The sample was immediately transferred back to the plate reader to begin a kinetic acquisition measuring the absorbance spectra from 300 to 500 nm at 25 °C every 2 min for 24 h. Subsequently, the same procedure was carried about with pNIPAM<sub>15</sub>-r-pDMAEA(Azo)<sub>1</sub> at an effective azobenzene concentration of 0.15 mM, again performed with and without 0.5 eq. CB[8].

**2.6.** Polymer Synthesis and Post-Synthetic Azobenzene Modification. The synthesis of random copolymers and their post-synthetic azobenzene modification (Scheme 2) proceeded as shown below.

2.6.1. Synthesis of pNIPAM<sub>x</sub>-r-pDMAEA<sub>1</sub>. Radical copolymerization with different ratios of N-isopropylacrylamide (NIPAM) to 2-(dimethylamino)ethyl acrylate (DMAEA) of 10:1, 15:1, 18:1, 20:1, and 30:1 was performed. As an example, the synthesis of the 15:1 ratio (pNIPAM<sub>15</sub>-r-pDMAEA<sub>1</sub>) is described: NIPAM (1.70 g), DMAEA (0.143 g), and azobis(isobutyronitrile) (AIBN, 7.0 mg) were dissolved in DMF (5 mL) in a Schlenk flask. The flask was vacuumed and backfilled with N<sub>2</sub> for three cycles before immersion in a 60 °C oil bath to thaw the solution and initiate polymerization. After 6 h, the reaction was quenched by exposure to air. The polymerization mixture was precipitated into diethyl ether three times. The product was obtained as fine white powder (1.62 g). Aqueous size exclusion chromatography was performed on a Thermo-Fisher instrument, eluting with 0.2 mL/min of 0.1 M NaN3 over a Shodex OHpak SB-804 HQ column (8 mm × 300 mm, 15 °C) using a REFRACTOMAX-521 detector to obtain molecular weight relative to a PEO calibration set. The actual ratio of NIPAM to DMAEA in

Scheme 2. Synthetic Procedure to Yield Azobenzene-Pendant Copolymers from (A) Radical Polymerization of Different Ratios of NIPAM:DMAEA (X:1) and (B) Modification of Synthesized Copolymer with AzoBr on DMAEA Side-Chains

synthesized copolymers was calculated by comparison of relevant integrations from  ${}^1H$  NMR spectrum in  $D_2O$ .

2.6.2. Synthesis of pNIPÂM<sub>X</sub>-r-pDMAEA(Azo)<sub>1</sub>. 4-Bromomethylphenyldiazenylanisole (AzoBr) was used to modify synthesized polymers with pendant azobenzenes for each ratio of NIPAM:D-MAEA. As an example, the synthesis of pNIPAM<sub>15</sub>-r-pDMAEA-(Azo)<sub>1</sub> proceeded as follows: AzoBr (0.25 g, 90% pure as stated above) and the synthesized copolymer (pNIPAM<sub>15</sub>-r-pDMAEA<sub>1</sub>, 1.20 g) were dissolved in THF (20 mL) and stirred for 3 days. The reaction mixture was precipitated into diethyl ether three times. The product was obtained as fine orange powder (1.35 g). The conversion of DMAEA side-chains to azobenzene pendants in the final copolymer was determined to be quantitative for all ratios by comparison of relevant signals from <sup>1</sup>H NMR spectrum in D<sub>2</sub>O.

**2.7. Temperature-Dependent Phase Transition.** NIPAM-containing polymers often exhibit a lower critical solution temperature (LCST) phase transition, which typically leads to a transition from translucent to opaque in polymer solutions. This gross transition was thus monitored visually for pNIPAM<sub>15</sub>-r-pDMAEA<sub>1</sub> compared to pNIPAM<sub>15</sub>-r-pDMAEA(Azo)<sub>1</sub> to determine the impact of azobenzene modification on apparent LCST properties. Solutions of both polymers were prepared at 5 mg/mL in DI water and were floated within a temperature-controlled water bath with constant stirring. After 10 min of equilibration at each selected temperature, samples were quickly removed and assessed for visual signs of a transition before being returned to the bath to continue heating to the next set point.

**2.8. Hydrogel Preparation.** To prepare hydrogels, 0.5 equiv of CB[8] was added relative to azobenzene on copolymers of each ratio. For example, to prepare hydrogels from pNIPAM<sub>15</sub>-r-pDMAEA-(Azo)<sub>1</sub>, the copolymer (0.67 g) was combined with CB[8] (207.6 mg) and the mixture was fully dissolved in water to form a 5 wt % viscous solution. This solution was allowed to equilibrate overnight in the dark to ensure homogeneous mixing. The solution was then flash-frozen in liquid nitrogen, lyophilized, and resuspended at 10 wt % in water. The resulting hydrogels were maintained overnight in the dark to ensure homogeneity prior to rheological testing or to further assess light-responsive behavior.

**2.9. Rheology.** Mechanical properties of the hydrogels were studied using TA Instruments Discovery HR-2 rheometer fitted with a Peltier stage. All measurements were performed using a 25 mm parallel plate geometry and, after trimming the gel to the size of the geometry used, a bead of silicone oil was applied using a pipet circumferentially at the gap between the upper plate and Peltier base so as to minimize sample drying during testing. Sample viscosity was measured for pNIPAM<sub>15</sub>-r-pDMAEA(Azo)<sub>1</sub> with and without

addition of CB[8], prepared as described above. "Zero-shear" viscosity measurements were conducted by slowly ramping the rate of applied steady-shear; viscosity over the range of shear rates for which this property was nominally constant (gel: ~1.7 to ~50 Hz; sol:  $\sim$ 5 to  $\sim$ 125 Hz) were averaged to determine the zero-shear viscosity for each sample. Strain sweep measurements from 0.1% to 200% were conducted at 100 rad/s frequency to identify the linear viscoelastic region. Frequency sweep measurements from 0.1 to 200 rad/s at 4, 20, and 37 °C were conducted at 2% strain, a value verified to be centered within in the linear viscoelastic region from strain sweeps. A temperature scan was conducted at constant frequency (either 80 rad/s or 200 rad/s) and strain (10%) from 4 to 37 °C. For in situ UV dissipation and healing measurements, a home-built quartz stage which housed radially positioned high-powered LED light sources was used. The tunable output for this device from its 365 nm LEDs was set to ~15 mW/cm<sup>2</sup>, and measurements were collected at a constant strain of 2% and frequency of 200 rad/s at room temperature (~20 °C). While our home-built quartz stage lacked explicit temperature control, any heat from the LED source was dissipated through an isothermal contact with the instrument Peltier plate to prevent heat transfer to the stage.

## 3. RESULTS AND DISCUSSION

3.1. CB[8]@AzoSM Ternary Complex. In order to probe homoternary complex formation of CB[8] with two identical azobenzene motifs, a model small molecule asymmetric azobenzene variant was envisioned (AzoSM) which bears a pendant quaternary amine on one side (Scheme 1, Figure 2A, Figure S1). This design was in accordance with the typical preference of CB[n]-class macrocycles to bind guests with adjacent positive charges that align with their electronegative carbonyl-fringed portal upon insertion<sup>43</sup> while also enabling charge separation by antiparallel guest arrangement within the portal, which has been shown to facilitate physical cross-linking of hydrogels by other homoternary complexes. 41 Indeed, 1H NMR performed on trans-AzoSM with 0.5 equiv of CB[8] revealed the characteristic upfield shift in both the aromatic  $(H_b, H_c, H_d, \text{ and } H_e)$  and pendant  $(H_a, H_b, \text{ and } H_g)$  azobenzene protons attributable to shielding arising from host-guest complex formation (Figure 2B). This finding supports formation of a homoternary complex between CB[8] and trans-AzoSM.

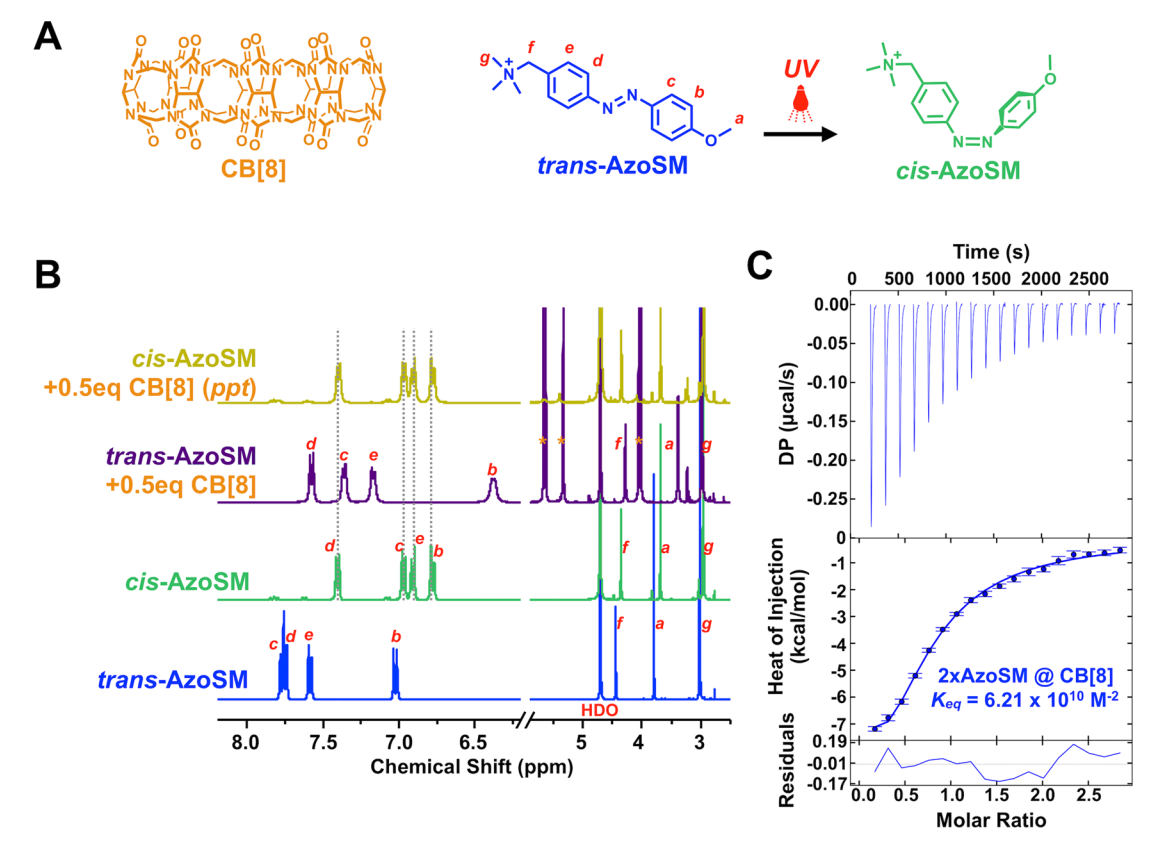


Figure 2. (A) Structures of CB[8] along with AzoSM in both its *trans*- and *cis*-isomeric state, with protons labeled for ease in interpreting shifts in  $^1$ H NMR. (B)  $^1$ H NMR in D<sub>2</sub>O for *trans*-AzoSM alone (*blue*), AzoSM alone following photoisomerization with UV irradiation (*green*), *trans*-AzoSM with 0.5 eq. CB[8] (*purple*), and AzoSM with 0.5 eq. CB[8] following photoisomerization with UV irradiation upon which a white CB[8] precipitate (*ppt*) is formed (*teal*). Proton assignments correspond to the labels in panel A, and \* denotes CB[8] protons. (C) Isothermal titration calorimetry (ITC), performed at 20 °C, with *trans*-AzoSM titrated into CB[8]. Heats of injection from n=3 separate experiments were fit simultaneously through global analysis to a sequential binding model, with residuals of the fit shown, to reveal the overall binding affinity ( $K_{eq}$ ) for the CB[8]–AzoSM homoternary complex.

In order to assess and further validate the stoichiometry and thermodynamics of the CB[8]-AzoSM homoternary complex, isothermal titration calorimetry (ITC) was performed with trans-AzoSM titrated into CB[8] in water (Figure 2C). The heats of injection from three independent experiments (n = 3)were fit though global analysis to a sequential binding model. The experiment performed at 20 °C yielded an overall binding constant  $(K_{eq})$  for the ternary complex of  $6.21 \times 10^{10}$  M<sup>-2</sup> with the first trans-AzoSM binding to CB[8] with an observed affinity  $(K_{a,l})$  of  $1.64 \times 10^6 \,\mathrm{M}^{-1}$ , while the second guest had an observed affinity  $(K_{a,2})$  of 3.79  $\times$  10<sup>4</sup> M<sup>-1</sup>. As such, the cooperativity factor  $(\alpha = K_{a,2}/K_{a,1})$  of the overall ternary complex was 0.02. Negative cooperativity is not unexpected given the relative size of the two guests as they assemble into their envisioned antiparallel arrangement to form a ternary complex within the CB[8] portal. ITC experiments were likewise performed at lower (4 °C) and higher (37 °C) temperatures, again in triplicate, which revealed the expected trend of a temperature-dependent reduction in affinity (Figure S2).

Subsequently, CB[8] binding was assessed upon photo-isomerization of **AzoSM** through irradiation with UV light. For **AzoSM** alone, conversion to its *cis* form resulted in an upfield shift in virtually all protons (Figure 2B), consistent with known shifts for azobenzene protons upon photoisomerization. <sup>35</sup> Following irradiation in the presence of 0.5 equiv of **CB**[8], the chemical shifts associated with **AzoSM** protons were

identical to cis-AzoSM alone. Also noteworthy, the signal attributed to CB[8] is conspicuously absent upon photoisomerization of AzoSM. When the <sup>1</sup>H NMR sample was examined closely, a chalk-white precipitate was clearly visible in the bottom of the tube immediately following UV irradiation (Figure S3). CB[8] is sparingly soluble in aqueous conditions  $(<10 \mu M)$ , 44,45 and therefore, the conditions used for NMR (15 mM AzoSM, 7.5 mM CB[8]) are well in excess of its solubility limit. Taken together, cis-AzoSM is presumed to have no appreciable binding to CB[8]. While prior reports have shown preferential formation of 1:1 complexes between CB[8] and certain *cis*-azobenzene variants, 35,39,46 in the present case, cis-AzoSM was not able to bind CB[8] to afford solubility to the otherwise insoluble macrocycle. This inability of cis-AzoSM to bind CB[8] is furthermore evidence that the trans-to-cis conversion happens for AzoSM when it is free in solution in the course of its dynamic exchange in binding to CB[8].

As mentioned previously, the *trans* state is commonly the thermodynamically preferred state for azobenzenes, and following photoisomerization to its *cis* form, most azobenzenes will subsequently undergo a *cis-to-trans* thermal relaxation over time or upon heating. Depending on design and/or substitution, the rate at which this process proceeds can vary from seconds to several days. <sup>47–49</sup> After the formation of *cis*-**AzoSM** with simultaneous precipitation of **CB**[8] was verified, the thermal relaxation of this molecule to its *trans* state was subsequently investigated. Interestingly, virtually no *cis-to-trans* 

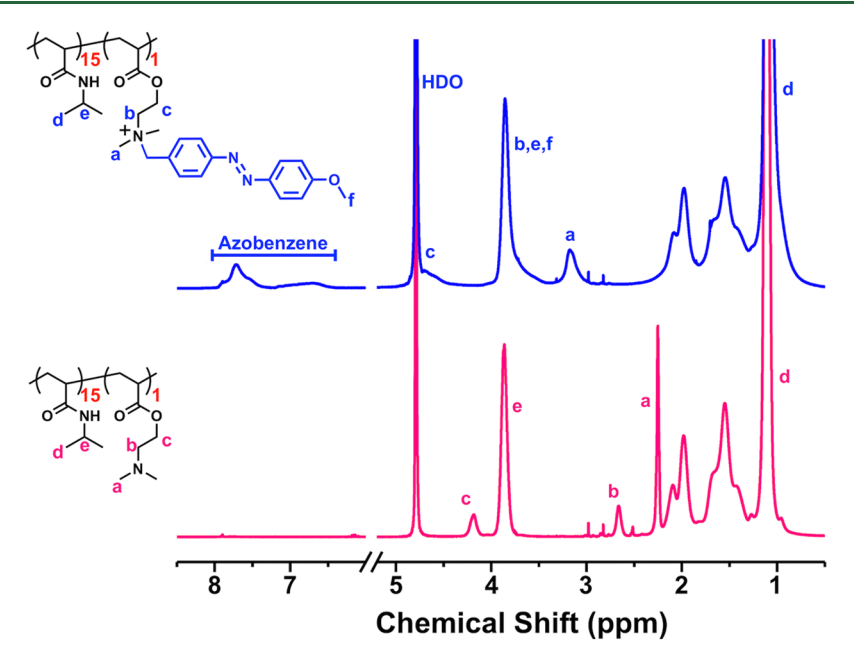


Figure 3. Post-synthetic azobenzene modification on pNIPAM<sub>15</sub>-r-pDMAEA<sub>1</sub>, verified to be quantitative by  $^{1}$ H NMR, with the spectra for the synthesized polymer (*bottom*) as well as that following modification with AzoBr as described (*top*). Protons are labeled according to the structures shown for ease in observing shifts. The quantitative conversion in this example trace is representative of all other polymer ratios (X:1) prepared.

relaxation was observed over the course of hours of observation at room temperature. Indeed, it was only after 24 h of incubation at 40 °C that AzoSM could be completely reversed back to its trans state (Figure S4) at the concentrations used in this <sup>1</sup>H NMR study (15 mM). Interestingly, even after such a long time, and under elevated temperatures, the CB[8] precipitate which had formed upon photoisomerization was sparingly resolubilized. In order to more closely study the kinetics of cis-to-trans relaxation of AzoSM, UV-vis absorbance spectroscopy was performed on dilute solutions (0.15 mM) before, and then continuously for 24 h following UV irradiation to induce photoisomerization (Figure S5). Indeed, the cis-to-trans reversal was nearly identical with and without addition of 0.5 equiv of CB[8], wherein room temperature recovery of trans-Azobenzene proceeded to ~20% in both cases. This supports a slow cisto-trans reversal of AzoSM which was not appreciably increased by the presence of CB[8].

3.2. Polymer Synthesis and Post-Synthetic Functionalization. After confirming homoternary complex formation between CB[8] and the asymmetric trans-AzoSM guest, copolymers were next designed to present this motif attached pendant from the polymer backbone. Two monomers, Nisopropylacrylamide (NIPAM) and 2-(dimethylamino)ethyl acrylate (DMAEA) were selected on the basis of their comparable reactivity for standard free-radical AIBN copolymerization (Scheme 2A). Random copolymers were synthesized with target NIPAM:DMAEA ratios of 10:1, 15:1, 18:1, 20:1, and 30:1 (pNIPAM<sub>x</sub>-r-pDMAEA<sub>1</sub>). Size-exclusion chromatography (SEC) was used to verify polymer molecular weight and determine polydispersity for each of the synthesized copolymers (Table 1, Figure S6), with all synthesized copolymers having  $M_p$  of ~22.3-32.3 kDa and PDI of ~1.85-2.45. Quantification of <sup>1</sup>H NMR for synthesized copolymers furthermore showed that monomer content of each copolymer was consistent with the input feed ratios of

Table 1. SEC and <sup>1</sup>H NMR Characterization of Synthesized Copolymers

Polymer	$M_{ m n}  m (kDa)$	PDI	NIPAM:DMAEA (¹H NMR)
pNIPAM <sub>10</sub> -r-pDMAEA <sub>1</sub>	22.3	1.85	10.41:1
pNIPAM <sub>15</sub> -r-pDMAEA <sub>1</sub>	27.8	2.45	15.16:1
$pNIPAM_{18}\text{-}r\text{-}pDMAEA_1$	27.1	2.17	17.79:1
$pNIPAM_{20}\text{-}r\text{-}pDMAEA_1$	23.3	2.12	20.32:1
${\rm pNIPAM_{30}\text{-}r\text{-}pDMAEA}_{1}$	32.3	2.32	29.58:1

NIPAM and DMAEA (Table 1, Figure S7), supporting the comparable reactivity of these two monomers.

Synthesized pNIPAM<sub>x</sub>-r-pDMAEA<sub>1</sub> copolymers were subsequently modified to afford an azobenzene side-chain. DMAEA groups were modified using a standard Menshutkin reaction with an alkyl halide (AzoBr), which was an intermediate from the synthesis of AzoSM (Scheme 1, Figure S1). This route afforded a pendant azobenzene resembling the AzoSM species connected via its quaternary amine (Scheme 2B). The modification of synthesized copolymers proceeded quantitatively for each copolymer ratio, with no unmodified DMAEA signals remaining by <sup>1</sup>H NMR for any of the ratios (Figure 3, Figure S8). Accordingly, this post-synthetic modification method yielded a series of pNIPAMx-r $pDMAEA(Azo)_1$ , with X = 10, 15, 18, 20, or 30. More generally, this modification approach enabled facile use of monomers with effectively identical reactivity to synthesize random copolymers by free-radical polymerization at defined ratios to subsequently install an azobenzene as a lightresponsive side-chain on the synthesized polymers. This approach, using AzoBr along with commercial tertiary amine-bearing monomers, should be extensible to the creation of other polymeric materials for subsequent installation of an azobenzene motif. The creation of copolymers from NIPAM groups has been shown to shift the phase transition temperature of resulting materials.<sup>50</sup> Notably, azobenzene modification led to an apparent LCST for pNIPAMx-r-

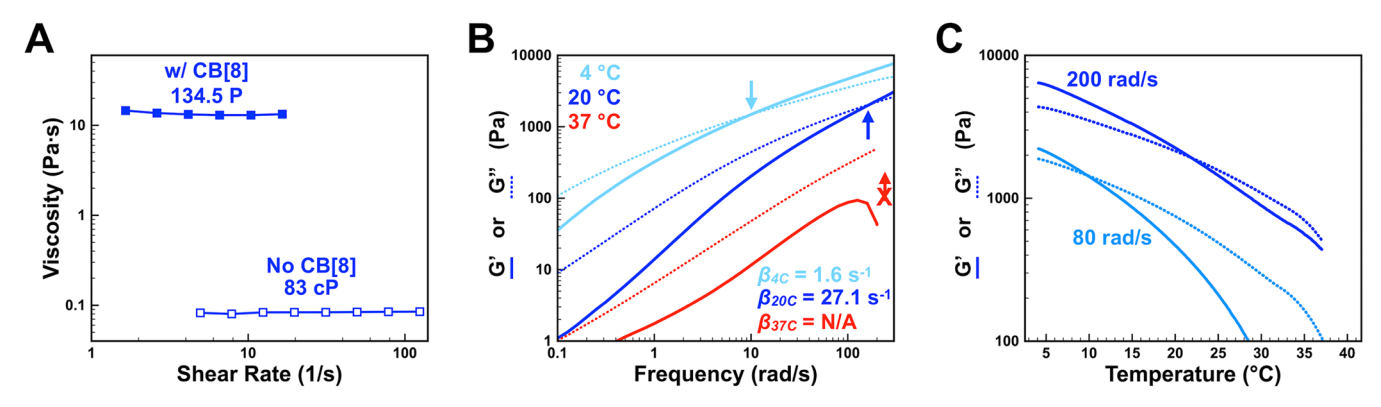


Figure 4. Rheological properties of supramolecular hydrogels prepared from pNIPAM<sub>15</sub>-r-pDMAEA(Azo)<sub>1</sub> and 0.5 eq of CB[8] per azobenzene on the polymer. (A) Zero-shear viscosity determination for the copolymer without CB[8] (*open squares*), as well as with CB[8] (*filled squares*). (B) Variable frequency rheology performed at 4 °C (*light blue*), 20 °C (*dark blue*), and 37 °C (*red*) at 2% strain. The bulk relaxation rate ( $\beta$ ), as determined the G'-G'' crossover (*arrows*) is shown for each trace. (C) Variable temperature rheology performed at 2% strain and a frequency of either 80 rad/s (*light blue*) or 200 rad/s (*dark blue*).

**pDMAEA**(**Azo**)<sub>1</sub> of between 45 and 50 °C compared to 30–35 °C for the **pNIPAM**<sub>x</sub>-**r**-**pDMAEA**<sub>1</sub> copolymer (Figure S9). The comparative light transmittance between the two samples following this phase change was also qualitatively different, with **pNIPAM**<sub>x</sub>-**r**-**pDMAEA**(**Azo**)<sub>1</sub> remaining translucent while **pNIPAM**<sub>x</sub>-**r**-**pDMAEA**<sub>1</sub> was fully opaque, suggesting larger aggregates in the latter material.

3.3. Supramolecular Hydrogel Formation. After first verifying the formation of CB[8]-AzoSM homoternary complexes of modest affinity, and subsequently affording the installation of azobenzene pendants to synthesized copolymers, CB[8] was next used to facilitate supramolecular hydrogel formation via ternary complex formation. The addition of CB[8] to pNIPAM<sub>x</sub>-r-pDMAEA(Azo)<sub>1</sub> copolymer solutions in water resulted in an increase in viscosity of 2+ orders of magnitude in all cases. For example, the zero-shear viscositywhich for shear-thinning hydrogels, such as these, is defined as the average viscosity value over its constant region at low shear rate in a steady-shear setup<sup>33</sup>—of pNIPAM<sub>15</sub>-r-pDMAEA-(Azo), in water increased from 83 cP to 13450 cP upon the addition of 0.5 equiv of CB[8] for each azobenzene on the polymer at 10 wt % total solids (Figure 4A). The magnitude of this increase is consistent with prior work using CB[8] ternary complexation for the physical cross-linking of guest-appended polymers.<sup>33</sup> A curious observation was realized from pNIPAM<sub>10</sub>-r-pDMAEA(Azo)<sub>1</sub> in these studies, as it remained turbid following the addition of CB[8] even after prolonged sonication as well as after months of equilibration (Figure S10). This was rationalized to result from CB[8] which was not fully soluble in the amount required to cross-link the guests of this polymer, given its higher ratio of pendant azobenzene groups. Furthermore, CB[8] steric effects resulting from a higher density of azobenzene cross-link sites may impede polymer chain flexibility and/or prevent CB[8] from accessing all available binding sites. It should also be noted that this copolymer had the lowest NIPAM content, which at ambient temperatures is expected to offer enhanced solubility relative to the azobenzene-modified group.

Given the large increase in viscosity for these samples, which also exhibited "self-supporting" character upon vial inversion typical of a supramolecular hydrogel, variable frequency oscillatory rheology was next performed to understand the dynamics of these hydrogels (Figure 4B, Figures S11 and S12). Due to its incomplete solubilization of CB[8], rheology of

pNIPAM<sub>10</sub>-r-pDMAEA(Azo)<sub>1</sub> was not considered reliable. All materials exhibited frequency-dependent G' behavior which is a hallmark of supramolecular hydrogels and arises from their dynamic physical cross-linking, and the viscosity of each polymer decreased with an increase in the oscillatory shear rate which is consistent with the typical behavior of shear-thinning supramolecular hydrogels. An interesting observation was made when evaluating the dynamic properties of these materials as a function of temperature. The initial design had included NIPAM monomers for its well-known thermoresponsive properties,<sup>51</sup> yet these materials exhibited substantial differences in their dynamic properties even at temperatures below the apparent phase transition of the azobenzenemodified copolymers (Figure S9). For example, the G'-G''crossover point, known as the bulk relaxation rate  $(\beta)$ , 33 shifted for pNIPAM<sub>15</sub>-r-pDMAEA(Azo)<sub>1</sub> from 1.6 Hz at 4 °C to 27.1 Hz at 20 °C. Limitations in the frequency rate for the instrument/geometry used did not allow for a determination of  $\beta$  at 37 °C in this sample.

The observed increase in relaxation rate revealed a network that was roughly 1+ order of magnitude more dynamic at 20 °C than it was at 4 °C. Given the relatively low  $K_{eq}$  for the CB[8]-AzoSM ternary complex found in ITC studies, it is presumed that this temperature-dependent increase in dynamics arises from a concomitant reduction in overall  $K_{ea}$ with increased temperature, as was found in temperaturedependent ITC studies for the small molecule AzoSM guest (Figure S2). Given the low-affinity binding observed for the second guest  $(K_{a,2})$  in these small molecule studies, it is reasonable to assume the reduction may be even more pronounced with a polymer-appended guest forcing a defined orientation for CB[8] insertion. Gel-to-sol transitions in CB[8]based supramolecular hydrogels upon increasing temperature have been previously observed and, in those cases, were also attributed to a reduction in  $K_{eq}$  with increased temperature.<sup>33</sup> It is at the same time noteworthy that the modulus value for this G'-G'' crossover point (~1450 Pa) is nearly identical when comparing samples at 4 and 20 °C; this indicates that at the frequency corresponding to the relaxation rate of the hydrogel at each temperature, the materials have effectively identical network topology. This finding further excludes phase transition behavior of NIPAM as the underlying cause of temperature-induced changes in dynamics for these materials, given that no such difference is expected when comparing 4

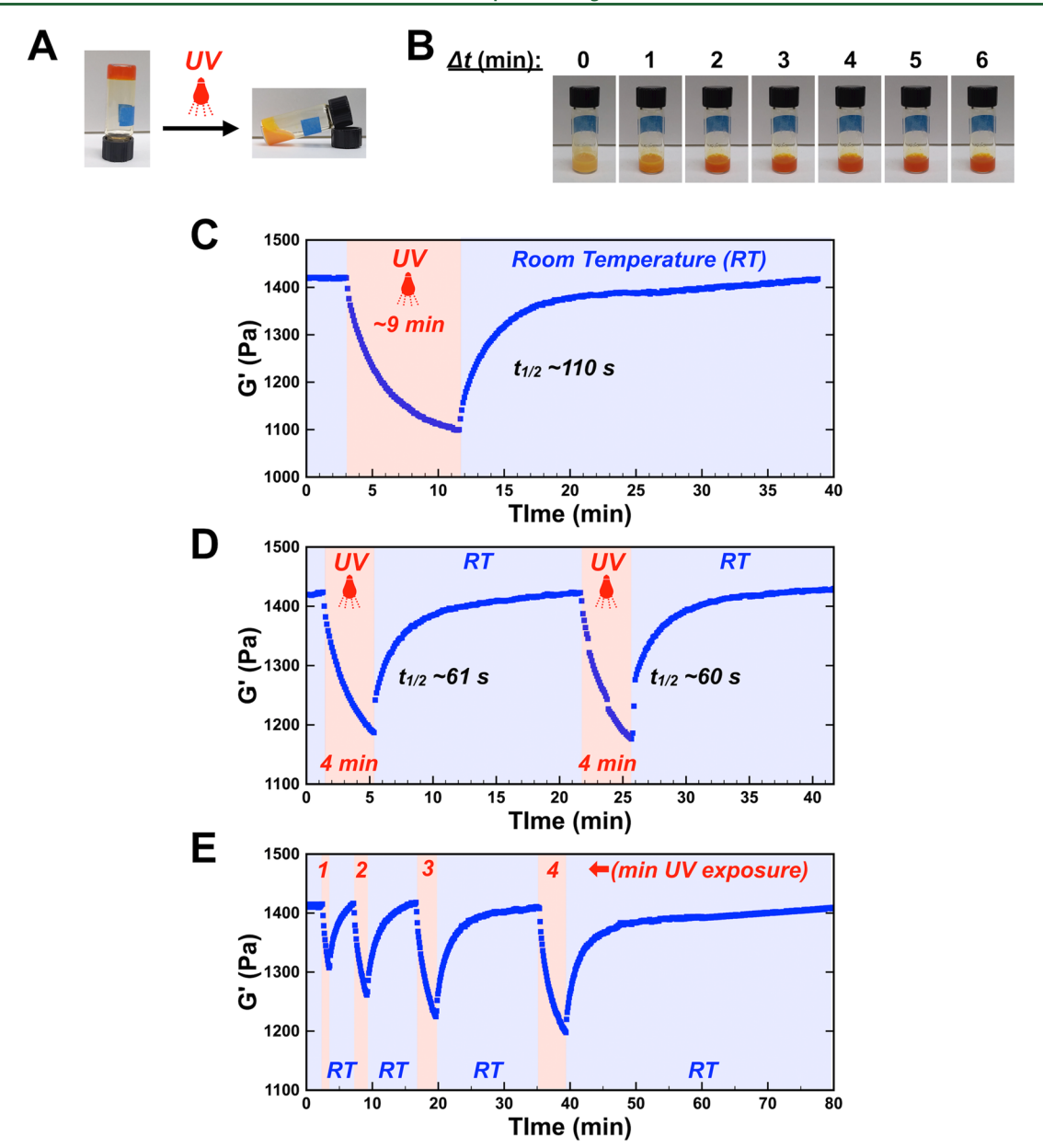


Figure 5. UV-responsive properties of hydrogels prepared from pNIPAM $_{15}$ -r-pDMAEA(Azo) $_1$  and 0.5 eq of CB[8] per azobenzene on the polymer. (A) Example *gel-to-sol* transition of the hydrogel upon exposure to UV light. (B) Photographs illustrating the time-course of relaxation and hydrogel recovery at room temperature following UV irradiation. (C–E) Rheology with *in situ* irradiation performed at 200 rad/s, 2% strain, and ~20 °C with irradiation (*red shaded*) followed by room temperature incubation (*blue shaded*), showing the half-life of recovery. G' is shown to highlight the impact of irradiation on reversibly reducing network topology.

and 20 °C; this was supported by studies which established an elevated LCST for azobenzene-modified copolymers (Figure S9). Accordingly, the importance of temperature-dependent reduction in  $K_{eq}$  of the supramolecular motif for the polymerappended guest likely drives the temperature-dependent change in properties of these hydrogel materials.

The gradual temperature-dependent reduction in G' and G'' as temperature is increased under constant frequency (Figure 4C) furthermore supports a temperature-dependent reduction in  $K_{eq}$ . A NIPAM phase transition would be thought to have a more dramatic temperature-dependent reduction in mechanical properties, as was observed in other supramolecular hydrogels. Though a G'-G'' crossover is indeed observed in this temperature scan, it is important to note that this feature does not indicate a thermal transition but instead is reflective

of the experiment being performed at a constant frequency. Thus, the crossover when the thermal ramp is performed at 200 rad/s is to the right of that when the thermal ramp is performed at 80 rad/s.

When comparing hydrogel dynamics as a function of relative monomer ratios, a general trend emerged wherein polymers with lower azobenzene substitution proved more dynamic (Figure S12). At 4 °C, the values of  $\beta$  increased from 1.6 Hz (X = 15) to 7.9 Hz (X = 18) to 15.1 Hz (X = 20) to 16.7 Hz (X = 30). Likewise, at 20 °C, the values of  $\beta$  increased from 27.1 Hz (X = 15) to 32.6 Hz (X = 18) to 41.4 Hz (X = 20). The  $\beta$  value for the X = 30 sample at 20 °C was not observable due to limits in the frequency rate for the instrument/geometry used. The observation of an increase in bulk relaxation rate with temperature, attributed to a reduction in  $K_{eq}$ , is thus

conserved across all copolymer ratios. This finding for an increase in  $\beta$  as the number of pendant azobenzene guests is reduced (i.e., as 'X' is increased) corresponds to prior findings wherein reducing the number of pendant supramolecular motifs led to hydrogel networks with faster relaxation dynamics. <sup>53</sup> It is also noteworthy that the modulus at which the G'-G'' crossover point occurs generally increases as a function of NIPAM content of the hydrogels and thus inversely to the extent of azobenzene modification on the copolymer. For instance, at 4 °C, the G'-G'' crossover occurred at 1450 Pa (X = 15), 1800 Pa (X = 18), 2100 Pa (X = 20), and 4800 Pa (X = 30). This effect may be attributable to NIPAM facilitating more chain bundling in the network.

Rapid swelling and material dissolution are possible concerns when working with supramolecular hydrogels which are dynamic and constructed from low-affinity interactions, especially in the context of their eventual use as injectable biomaterials. Accordingly, the stability of hydrogels prepared from pNIPAM<sub>15</sub>-r-pDMAEA(Azo)<sub>1</sub> with CB[8] was explored under dilution (Figure S13). Of note, this hydrogel swelled to ~2.5 times its initial volume while maintaining its structure over 24 h. By 48 h, the gel had begun to erode, and by 72 h, the gel structure was no longer intact. One point to emphasize here is that hydrogels which swell and erode in under 24 h by this same study have been shown to persist in subcutaneous space *in vivo* for over 1 month.<sup>14</sup> As such, the swelling and erosion seen here will not necessarily prove inhibitory to the eventual in vivo use of this material, provided that suitable modification can be identified to enable gel formation at physiologic temperatures.

3.4. Light-Responsive Dissipation and Spontaneous **Sol**–**Gel Recovery.** The primary motivation for evaluating the feasibility of azobenzene-based CB[8] homoternary complexes was to leverage azobenzene photoisomerization to yield hydrogels responsive to an external light stimulus. After 10 min of UV irradiation of hydrogels prepared at 10 wt % from pNIPAM<sub>15</sub>-r-pDMAEA(Azo)<sub>1</sub> with 0.5 equiv of CB[8] per azobenzene on the copolymer, the formed hydrogel underwent a gel-to-sol transition as evidenced by the material flowing upon vial inversion (Figure 5A). The sol in this case was turbid yellow and very viscous, with evident formation of a chalkwhite CB[8] precipitate suspended in the sol. Given the very slow thermal relaxation previously observed for AzoSM after being converted to its cis form (Figures S3 and S4), as well as the practically irreversible precipitation of CB[8] in this prior sample, it was not expected that these hydrogels would recover their properties. It was thus very surprising that, following UV irradiation, the sample underwent a sol-gel transition within minutes while sitting on the bench at room temperature (Figure 5B, Movie S1). The turbid light-yellow sol quickly recovered its bright orange and translucent character within minutes.

Rheology was subsequently performed with *in situ* irradiation to verify the kinetics of network recovery following its UV-induced disruption (Figure 5C–E). As was observed visually for the bulk sample on the bench, following disruption of the network by UV light, the original network topology (e.g., G') could be restored within minutes of cessation of irradiation, with a half-life of recovery of ~110 s when irradiation was performed for ~9 min (Figure 5C). In addition, the hydrogel was able to recover from repeated 4 min UV cycles with comparable recovery half-lives of ~60 s each time (Figure 5D). The "dose" of applied light impacted both the

extent of network disruption as well as the kinetics of network recovery, as demonstrated when exposure time was sequentially applied for 1, 2, 3, and 4 min (Figure 5E). It is noted that G' following prolonged irradiation was still on the order of  $\sim 1100$  Pa, well above what would be expected for a non-cross-linked polymer solution. This is reasoned to arise from the presence of CB[8] precipitates which offer some network connectively though surface adsorption of polymer chains, similar to what has been shown for systems of polymer—nanoparticle hydrogels. Though these interactions increased viscosity here, they were at the same time not sufficient to limit flow of the post-UV-treated material.

The difference in recovery behavior for polymer-appended azobenzene compared to that of the model AzoSM molecule remains to be more fully explored, as does the difference in CB[8] precipitation and resolubilization in the two systems. UV-vis studies were performed to explore the impact of polymer appendage of this particular azobenzene on its rate of thermal relaxation (Figure S14). A dilute solution of pNIPAM<sub>15</sub>-r-pDMAEA<sub>1</sub> did not show any acceleration of azobenzene relaxation for its cis to trans state relative to AzoSM, again yielding approximately 20% recovery of the trans form after 24 h. However, the addition of 0.5 eq CB[8] accelerated cis-trans thermal relaxation for pNIPAM<sub>15</sub>-rpDMAEA1 compared to what had been observed for AzoSM. In this dilute case, the cis to trans reversal was effectively complete over 24 h. Thermal relaxation may thus be "catalyzed" by a preference for CB[8] to bind this particular azobenzene in its trans form when polymer-appended; a related, yet opposite, observation was observed for a particular azobenzene which preferred binding CB[7] in its cis form. 55 It seems likely that CB[8] is able to catalyze the reversal to the trans- state specifically for the polymer-appended variant of this azobenzene. While this process takes  $\sim$ 24 h to complete in the dilute condition of UV-vis, the much higher concentration of CB[8] and azobenzene in the hydrogel could drive this reversal to progress more quickly. This finding is likely due to the relatively weak binding affinity of the trans version of this azobenzene requiring high concentration to drive equilibrium toward the bound state, thus explaining the difference in kinetics of these two dramatically different concentration regimes. The CB[8], for its part, may not form the same large precipitates in the presence of a viscous polymer as it does in solution phase, and thus may be more rapidly resolubilized upon the return of its preferred trans-azobenzene guest.

## 4. CONCLUSIONS

Supramolecular hydrogels have been increasingly used for a number of different applications, with particular benefits in the context of easily injectable biomaterials and drug delivery devices. The dynamics of underlying host-guest physical cross-linking mechanisms used to create many variations of these materials enable the formation of hydrogels which can relax in response to an applied stress and self-heal following formation of a defect or disruption of the network. In terms of routes to achieve physical cross-linking and hydrogel formation, the CB[8] macrocycle motif offers particular appeal for its uncommon ability to simultaneously bind two guests within its portal, though it has some drawbacks in terms of its limited water solubility. For the further expansion of the properties and utility of host-guest supramolecular materials, stimuli-responsive functionality is a topic of great interest. Light is an important stimulus in this regard, as it can be locally

applied with controlled intensity and duration of exposure. Toward actuating a light stimulus to drive reversible changes in supramolecular material properties, azobenzene motifs have been commonly used as guests. Yet, the use of azobenzene as a guest to facilitate CB[8]-mediated physical cross-linking and hydrogel formation has yet to be reported.

Here, an asymmetric azobenzene is explored which is capable of forming homoternary complexes with CB[8] having modest affinity. Then, using standard free-radical polymerization techniques with defined ratios of commercially available monomers, copolymers were prepared which could be post-synthetically modified to present pendant azobenzenes by facile, quantitative, and extensible methodology. The resulting copolymers, when combined with CB[8], exhibited traits common of supramolecular hydrogels, particularly in their dynamic properties arising from underlying dynamics of host—guest physical cross-linking interactions, which were further found to be dictated by temperature. Upon UV irradiation, these hydrogels underwent a *gel-to-sol* transition. However, and quite surprisingly, the gel form was restored within minutes of ceasing irradiation.

This general approach, though here limited by the modest and temperature-dependent affinity of the CB[8]—azobenzene homoternary complex as well as the limited solubility of CB[8] when free in solution, still reveals a number of interesting features and design rules to inform and enhance future application of this class of materials. For use at body temperature, the azobenzene forming the homoternary complex may be redesigned to achieve higher affinity. Alternatively, a heteroternary complex with another guest which binds at higher affinity and/or is less sterically limited may be explored.

While the current study establishes the utility of lightresponsive ternary cross-linking in supramolecular hydrogels, there are a variety of biomaterial contexts for which this technique could be deployed to enable new responsive hydrogel platforms. Indeed, many applications may be enhanced by the autonomous thermal relaxation of the azobenzene guest driving hydrogel network recovery which was observed here following application of a UV stimulus. Transient hydrogel network disruption and subsequent recovery may afford a strategy to briefly alter the mechanics or network topology of a material as a synthetic extracellular matrix, enabling precise external control over these properties to dictate function or phenotype of adhered cells. In addition, a light stimulus may be used to temporarily disrupt a hydrogel network for triggered and short-term burst release of an encapsulated macromolecular therapeutic payload, with the network quickly recovering to cease its release within minutes of applying the trigger. In future iterations of this technology, a focus on enhancing the underlying supramolecular interactions of the hydrogel to afford stable cross-linking at physiologic temperatures will allow application-specific targets for these materials to be more thoroughly explored as new biomaterials and drug delivery devices.

## ASSOCIATED CONTENT

## **Supporting Information**

The Supporting Information is available free of charge at https://pubs.acs.org/doi/10.1021/acs.biomac.0c00950.

<sup>1</sup>H NMR of AzoSM precursors, ITC data for CB[8]—AzoSM at 4°C, NMR tube containing *cis*-AzoSM and

CB[8] precipitate, H NMR exploring thermal *cis-to-trans* relaxation for AzoSM w/ CB[8], UV—vis for *cis-to-trans* relaxation for AzoSM w/ and w/o CB[8], SEC trace of synthesized pNIPAM<sub>x</sub>-r-pDMAEA<sub>1</sub> copolymers, <sup>1</sup>H NMR of synthesized pNIPAM<sub>x</sub>-r-pDMAEA<sub>1</sub> copolymers, <sup>1</sup>H NMR for azobenzene modification of pNIPAM<sub>x</sub>-r-pDMAEA(Azo)<sub>1</sub> copolymers, gross assessment of LCST for polymers before and after azobenzene modification, photograph of CB[8] insolubility in pNIPAM<sub>10</sub>-r-pDMAEA(Azo)<sub>1</sub>, frequency-dependent complex viscosity of pNIPAM<sub>15</sub>-r-pDMAEA(Azo)<sub>1</sub> hydrogels w/ CB[8], rheology for other copolymer ratios, hydrogel swelling and dissolution into H<sub>2</sub>O, UV—vis for *cis-to-trans* relaxation of pNIPAM<sub>15</sub>-r-pDMAEA(Azo)<sub>1</sub> w/ & w/o CB[8] (PDF)

Thermal relaxation and hydrogel recovery (MP4)

#### AUTHOR INFORMATION

#### **Corresponding Author**

Matthew J. Webber — University of Notre Dame, Department of Chemical & Biomolecular Engineering, Notre Dame, Indiana 46556, United States; orcid.org/0000-0003-3111-6228; Email: mwebber@nd.edu

#### **Authors**

Lei Zou — University of Notre Dame, Department of Chemical & Biomolecular Engineering, Notre Dame, Indiana 46556, United States

Christopher J. Addonizio — University of Notre Dame, Department of Chemical & Biomolecular Engineering, Notre Dame, Indiana 46556, United States

Bo Su — University of Notre Dame, Department of Chemical & Biomolecular Engineering, Notre Dame, Indiana 46556, United States

Matthew J. Sis — University of Notre Dame, Department of Chemical & Biomolecular Engineering, Notre Dame, Indiana 46556, United States

Adam S. Braegelman — University of Notre Dame, Department of Chemical & Biomolecular Engineering, Notre Dame, Indiana 46556, United States

**Dongping Liu** – University of Notre Dame, Department of Chemical & Biomolecular Engineering, Notre Dame, Indiana 46556, United States

Complete contact information is available at: https://pubs.acs.org/10.1021/acs.biomac.0c00950

#### Notes

The authors declare no competing financial interest.

## ■ ACKNOWLEDGMENTS

M.J.W. acknowledges funding support from the National Science Foundation (DMR-BMAT CAREER award 1944875), a 3M Non-Tenured Faculty Award (3M Company), and the University of Notre Dame "Advancing our Vision" initiative. The authors are grateful to the ND Energy Materials Characterization Facility for use of the rheometer and to the Biophysics Instrumentation Facility for use of the ITC.

#### REFERENCES

(1) Appel, E. A.; del Barrio, J.; Loh, X. J.; Scherman, O. A. Supramolecular polymeric hydrogels. *Chem. Soc. Rev.* **2012**, *41* (18), 6195–214.

- (2) Du, X.; Zhou, J.; Shi, J.; Xu, B. Supramolecular Hydrogelators and Hydrogels: From Soft Matter to Molecular Biomaterials. *Chem. Rev.* **2015**, *115* (24), 13165–307.
- (3) Webber, M. J.; Appel, E. A.; Meijer, E. W.; Langer, R. Supramolecular biomaterials. *Nat. Mater.* **2016**, *15* (1), 13–26.
- (4) Webber, M. J.; Langer, R. Drug delivery by supramolecular design. Chem. Soc. Rev. 2017, 46 (21), 6600-6620.
- (5) Rodell, C. B.; Mealy, J. E.; Burdick, J. A. Supramolecular Guest-Host Interactions for the Preparation of Biomedical Materials. *Bioconjugate Chem.* **2015**, *26* (12), 2279–89.
- (6) Mantooth, S. M.; Munoz-Robles, B. G.; Webber, M. J. Dynamic Hydrogels from Host-Guest Supramolecular Interactions. *Macromol. Biosci.* **2019**, *19* (1), No. e1800281.
- (7) Rodell, C. B.; Kaminski, A. L.; Burdick, J. A. Rational design of network properties in guest-host assembled and shear-thinning hyaluronic acid hydrogels. *Biomacromolecules* **2013**, *14* (11), 4125–34.
- (8) Highley, C. B.; Rodell, C. B.; Burdick, J. A. Direct 3D Printing of Shear-Thinning Hydrogels into Self-Healing Hydrogels. *Adv. Mater.* **2015**, 27 (34), 5075–9.
- (9) Sahoo, J. K.; VandenBerg, M. A.; Webber, M. J. Injectable network biomaterials via molecular or colloidal self-assembly. *Adv. Drug Delivery Rev.* **2018**, *127*, 185–207.
- (10) Nguyen, K. T.; West, J. L. Photopolymerizable hydrogels for tissue engineering applications. *Biomaterials* **2002**, 23 (22), 4307–14.
- (11) Van Tomme, S. R.; Storm, G.; Hennink, W. E. In situ gelling hydrogels for pharmaceutical and biomedical applications. *Int. J. Pharm.* **2008**, 355 (1–2), 1–18.
- (12) Phelps, E. A.; Enemchukwu, N. O.; Fiore, V. F.; Sy, J. C.; Murthy, N.; Sulchek, T. A.; Barker, T. H.; Garcia, A. J. Maleimide cross-linked bioactive PEG hydrogel exhibits improved reaction kinetics and cross-linking for cell encapsulation and in situ delivery. *Adv. Mater.* **2012**, 24 (1), 64–70 2.
- (13) Ahadian, S.; Sadeghian, R. B.; Salehi, S.; Ostrovidov, S.; Bae, H.; Ramalingam, M.; Khademhosseini, A. Bioconjugated Hydrogels for Tissue Engineering and Regenerative Medicine. *Bioconjugate Chem.* **2015**, 26 (10), 1984–2001.
- (14) Zou, L.; Braegelman, A. S.; Webber, M. J. Dynamic Supramolecular Hydrogels Spanning an Unprecedented Range of Host-Guest Affinity. ACS Appl. Mater. Interfaces 2019, 11 (6), 5695–5700.
- (15) Jeong, B.; Kim, S. W.; Bae, Y. H. Thermosensitive sol-gel reversible hydrogels. *Adv. Drug Delivery Rev.* **2002**, *54* (1), 37–51.
- (16) Zou, L.; Su, B.; Addonizio, C. J.; Pramudya, I.; Webber, M. J. Temperature-Responsive Supramolecular Hydrogels by Ternary Complex Formation with Subsequent Photo-Cross-linking to Alter Network Dynamics. *Biomacromolecules* **2019**, 20 (12), 4512–4521.
- (17) Zou, L.; Braegelman, A. S.; Webber, M. J. Spatially Defined Drug Targeting by in Situ Host—Guest Chemistry in a Living Animal. *ACS Cent. Sci.* **2019**, *5* (6), 1035—1043.
- (18) Yan, X.; Wang, F.; Zheng, B.; Huang, F. Stimuli-responsive supramolecular polymeric materials. *Chem. Soc. Rev.* **2012**, *41* (18), 6042–65.
- (19) Webber, M. J. Engineering responsive supramolecular biomaterials: Toward smart therapeutics. *Bioeng Transl Med.* **2016**, 1 (3), 252–266.
- (20) Montero de Espinosa, L.; Meesorn, W.; Moatsou, D.; Weder, C. Bioinspired Polymer Systems with Stimuli-Responsive Mechanical Properties. *Chem. Rev.* **2017**, *117* (20), 12851–12892.
- (21) Braegelman, A. S.; Webber, M. J. Integrating Stimuli-Responsive Properties in Host-Guest Supramolecular Drug Delivery Systems. *Theranostics* **2019**, *9* (11), 3017–3040.
- (22) Hoque, J.; Sangaj, N.; Varghese, S. Stimuli-Responsive Supramolecular Hydrogels and Their Applications in Regenerative Medicine. *Macromol. Biosci.* **2019**, *19* (1), 1800259.
- (23) Beharry, A. A.; Sadovski, O.; Woolley, G. A. Azobenzene Photoswitching without Ultraviolet Light. *J. Am. Chem. Soc.* **2011**, *133* (49), 19684–19687.

- (24) Wang, D.; Zhao, W.; Wei, Q.; Zhao, C.; Zheng, Y. Photoswitchable Azobenzene/Cyclodextrin Host-Guest Complexes: From UV- to Visible/Near-IR-Light-Responsive Systems. *ChemPhotoChem.* **2018**, 2 (5), 403–415.
- (25) Bandara, H. M. D.; Burdette, S. C. Photoisomerization in different classes of azobenzene. *Chem. Soc. Rev.* **2012**, *41* (5), 1809–1825
- (26) Yoshinori, T.; Tomofumi, N.; Masahiko, M.; Yoshinori, K.; Hiroyasu, Y.; Akira, H. Complex Formation and Gelation between Copolymers Containing Pendant Azobenzene Groups and Cyclodextrin Polymers. *Chem. Lett.* **2004**, 33 (7), 890–891.
- (27) Zhao, Y.-L.; Stoddart, J. F. Azobenzene-Based Light-Responsive Hydrogel System. *Langmuir* **2009**, 25 (15), 8442–8446.
- (28) Tamesue, S.; Takashima, Y.; Yamaguchi, H.; Shinkai, S.; Harada, A. Photoswitchable Supramolecular Hydrogels Formed by Cyclodextrins and Azobenzene Polymers. *Angew. Chem., Int. Ed.* **2010**, 49 (41), 7461–7464.
- (29) Kim, J.; Jung, I. S.; Kim, S. Y.; Lee, E.; Kang, J. K.; Sakamoto, S.; Yamaguchi, K.; Kim, K. New cucurbituril homologues: Syntheses, isolation, characterization, and X-ray crystal structures of cucurbit-[n]uril (n = 5, 7, and 8). *J. Am. Chem. Soc.* **2000**, *122* (3), 540–541.
- (30) Barrow, S. J.; Kasera, S.; Rowland, M. J.; del Barrio, J.; Scherman, O. A. Cucurbituril-Based Molecular Recognition. *Chem. Rev.* **2015**, *115* (22), 12320–406.
- (31) Lee, J. W.; Kim, K.; Choi, S.; Ko, Y. H.; Sakamoto, S.; Yamaguchi, K.; Kim, K. Unprecedented host-induced intramolecular charge-transfer complex formation. *Chem. Commun.* **2002**, No. 22, 2692–2693.
- (32) Ko, Y. H.; Kim, K.; Kang, J. K.; Chun, H.; Lee, J. W.; Sakamoto, S.; Yamaguchi, K.; Fettinger, J. C.; Kim, K. Designed self-assembly of molecular necklaces using host-stabilized charge-transfer interactions. *J. Am. Chem. Soc.* **2004**, *126* (7), 1932–1933.
- (33) Appel, E. A.; Biedermann, F.; Rauwald, U.; Jones, S. T.; Zayed, J. M.; Scherman, O. A. Supramolecular cross-linked networks via host-guest complexation with cucurbit[8]uril. *J. Am. Chem. Soc.* **2010**, *132* (40), 14251–60.
- (34) Appel, E. A.; Forster, R. A.; Koutsioubas, A.; Toprakcioglu, C.; Scherman, O. A. Activation energies control the macroscopic properties of physically cross-linked materials. *Angew. Chem., Int. Ed.* **2014**, *53* (38), 10038–43.
- (35) del Barrio, J.; Horton, P. N.; Lairez, D.; Lloyd, G. O.; Toprakcioglu, C.; Scherman, O. A. Photocontrol over cucurbit[8]uril complexes: stoichiometry and supramolecular polymers. *J. Am. Chem. Soc.* **2013**, *135* (32), 11760–3.
- (36) Zhao, J.; Zhang, Y. M.; Sun, H. L.; Chang, X. Y.; Liu, Y. Multistimuli-responsive supramolecular assembly of cucurbituril/cyclodextrin pairs with an azobenzene-containing bispyridinium guest. *Chem. Eur. J.* **2014**, *20* (46), 15108–15.
- (37) Ma, N.; Wang, W. J.; Chen, S.; Wang, X. S.; Wang, X. Q.; Wang, S. B.; Zhu, J. Y.; Cheng, S. X.; Zhang, X. Z. Cucurbit[8]uril-mediated supramolecular photoswitching for self-preservation of mesoporous silica nanoparticle delivery system. *Chem. Commun.* **2015**, *51* (65), 12970–3.
- (38) Del Barrio, J.; Ryan, S. T.; Jambrina, P. G.; Rosta, E.; Scherman, O. A. Light-Regulated Molecular Trafficking in a Synthetic Water-Soluble Host. *J. Am. Chem. Soc.* **2016**, *138* (18), 5745–8.
- (39) Tan, C. S. Y.; del Barrio, J.; Liu, J.; Scherman, O. A. Supramolecular polymer networks based on cucurbit[8]uril host—guest interactions as aqueous photo-rheological fluids. *Polym. Chem.* **2015**, *6* (44), 7652–7657.
- (40) Stappert, K.; Muthmann, J.; Spielberg, E. T.; Mudring, A.-V. Azobenzene-Based Organic Salts with Ionic Liquid and Liquid Crystalline Properties. *Cryst. Growth Des.* **2015**, *15* (9), 4701–4712.
- (41) Zou, L.; Webber, M. J. Reversible hydrogel dynamics by physical-chemical crosslink photoswitching using a supramolecular macrocycle template. *Chem. Commun.* **2019**, *55* (67), 9931–9934.
- (42) Brautigam, C. A.; Zhao, H.; Vargas, C.; Keller, S.; Schuck, P. Integration and global analysis of isothermal titration calorimetry data

for studying macromolecular interactions. *Nat. Protoc.* **2016**, 11 (5), 882–894.

- (43) Huang, Z.; Qin, K.; Deng, G.; Wu, G.; Bai, Y.; Xu, J.-F.; Wang, Z.; Yu, Z.; Scherman, O. A.; Zhang, X. Supramolecular Chemistry of Cucurbiturils: Tuning Cooperativity with Multiple Noncovalent Interactions from Positive to Negative. *Langmuir* **2016**, 32 (47), 12352–12360.
- (44) Lee, J. W.; Samal, S.; Selvapalam, N.; Kim, H. J.; Kim, K. Cucurbituril homologues and derivatives: New opportunities in supramolecular chemistry. *Acc. Chem. Res.* **2003**, *36* (8), 621–630.
- (45) Lagona, J.; Mukhopadhyay, P.; Chakrabarti, S.; Isaacs, L. The cucurbit[n]uril family. *Angew. Chem., Int. Ed.* **2005**, *44* (31), 4844–70.
- (46) Huang, H.; Juan, A.; Katsonis, N.; Huskens, J. Competitive inclusion of molecular photo-switches in host cavities. *Tetrahedron* **2017**, 73 (33), 4913–4917.
- (47) Garcia-Amoros, J.; Sanchez-Ferrer, A.; Massad, W. A.; Nonell, S.; Velasco, D. Kinetic study of the fast thermal cis-to-trans isomerisation of para-, ortho- and polyhydroxyazobenzenes. *Phys. Chem. Chem. Phys.* **2010**, *12* (40), 13238–13242.
- (48) Beharry, A. A.; Woolley, G. A. Azobenzene photoswitches for biomolecules. *Chem. Soc. Rev.* **2011**, *40* (8), 4422–37.
- (49) Bujak, K.; Orlikowska, H.; Malecki, J. G.; Schab-Balcerzak, E.; Bartkiewicz, S.; Bogucki, J.; Sobolewska, A.; Konieczkowska, J. Fast dark cis-trans isomerization of azopyridine derivatives in comparison to their azobenzene analogues: Experimental and computational study. *Dyes Pigm.* **2019**, *160*, 654–662.
- (50) Maeda, T.; Kanda, T.; Yonekura, Y.; Yamamoto, K.; Aoyagi, T. Hydroxylated Poly(N-isopropylacrylamide) as Functional Thermoresponsive Materials. *Biomacromolecules* **2006**, *7* (2), 545–549.
- (51) Heskins, M.; Guillet, J. E. Solution Properties of Poly(N-isopropylacrylamide). *J. Macromol. Sci., Chem.* **1968**, 2 (8), 1441–1455.
- (52) Kretschmann, O.; Choi, S. W.; Miyauchi, M.; Tomatsu, I.; Harada, A.; Ritter, H. Switchable Hydrogels Obtained by Supramolecular Cross-Linking of Adamantyl-Containing LCST Copolymers with Cyclodextrin Dimers. *Angew. Chem., Int. Ed.* **2006**, 45 (26), 4361–4365.
- (53) Rodell, C. B.; Kaminski, A. L.; Burdick, J. A. Rational Design of Network Properties in Guest—Host Assembled and Shear-Thinning Hyaluronic Acid Hydrogels. *Biomacromolecules* **2013**, *14* (11), 4125—4134.
- (54) Appel, E. A.; Tibbitt, M. W.; Webber, M. J.; Mattix, B. A.; Veiseh, O.; Langer, R. Self-assembled hydrogels utilizing polymer–nanoparticle interactions. *Nat. Commun.* **2015**, *6*, 6295.
- (55) Wu, J.; Isaacs, L. Cucurbit[7]uril Complexation Drives Thermal trans—cis-Azobenzene Isomerization and Enables Colorimetric Amine Detection. *Chem. Eur. J.* **2009**, *15* (43), 11675—11680.